Small-Angle and Wide-Angle X-ray Analyses of Syndiotactic Poly(vinyl alcohol) Microfibrils

Won Seok Lyoo*

School of Textiles and Regional Research Center, Yeungnam University, Kyongsan 712-749, Korea

Sergei Chvalun

Department of Polymer Structure, Karpov Institute of Physical Chemistry, 103064 Moscow, Ul, Vorontzovo, Pole 10, Russia

Han Do Ghim and Jae Pil Kim

School of Materials Science and Engineering, Seoul National University, Seoul 151-742, Korea

John Blackwell

Department of Macromolecular Science, Case Western Reserve University, Cleveland, Ohio 44106-7202

Received September 19, 2000; Revised Manuscript Received January 23, 2001

ABSTRACT: The crystal and microstructures of the novel microfibrillar poly(vinyl alcohol) fibers (PVA fibrils) having different syndiotactic diad (S-diad) contents of 56−65% have been investigated by small- and wide-angle X-ray methods. The PVA fibrils were directly prepared from the saponification and in-situ fibrillation without spinning procedure. Small-angle X-ray scattering data show that these PVA fibrils had various microvoid structures due to different stereoregularities, which was similar to those found in various natural cellulose fibers. Also, the higher the syndiotacticity was, the more regular and elongated the microvoids in PVA fibril were. This might be explained by a better alignment of PVA chains with higher syndiotacticity. To effectively orient the molecular chains of high molecular weight syndiotactic PVA fibril, a high-temperature zone drawing technique was applied. Degree of crystal orientation up to 0.991 was achieved by stretching the PVA fibril with S-diad content of 63.1% and with original degree of crystal orientation of 0.887 at around 250 °C close to its melting temperature. The maximum draw ratio of the PVA fibril increased with a decrease in the S-diad content, indicating that the crystal was more stable in higher syndiotactic PVA. When the same draw ratio was applied to the fibrils, higher crystal orientation was achieved for the fibrils having higher syndiotacticity. The crystallinity, the apparent lateral and longitudinal crystal sizes, and the crystal to amorphous length in long period of drawn PVA fibrils were larger in higher syndiotacticity. It turns out that PVA fibril drawn at 230 °C had a well-oriented lamellar structure. Moreover, dimensions of these lamellae were enlarged with increasing syndiotacticity.

Introduction

As a flexible chain polymer for the production of high performance fiber, high molecular weight (HMW) syndiotactic poly(vinyl alcohol) (PVA), whose mechanical and physical properties are much superior to those of atactic ones,[1−12] has received considerable attention. The commercial and scientific interests in this polymer arise from the fact that crystal lattice modulus of PVA along the chain direction is estimated over 250 GPa.[13,14] However, the major drawbacks of this material for the preparation of high strength and high modulus fibrous substances are as follows: One is the necessity of complicated processes of manufacture such as dissolving polymer, determining initial optimum spinning concentration, spinning, drawing, heat treatment, etc. The other is the difficulty in fully molecular orientation owing to the strong intermolecular hydrogen bonds between the adjacent hydroxyl groups in syndiotactic PVA.[15] Hence, the derivation of a new fiber forming method (fibrillation) for HMW syndiotactic PVA, not a conventional spinning process, is required.

* To whom correspondence should be addressed. Telephone 82-53-810-2532; Fax 82-53-811-2735; E-mail wslyoo@yu.ac.kr.

Recently, Lyoo et al.[3,4,6−9,16,17] reported that a well-oriented microfibrillar PVA fiber (PVA fibril) has been formed during saponification of poly(vinyl pivalate) (PVPi) or P(VPi/vinyl acetate) copolymer. This is true only for a syndiotactic precursor of PVA but not possible with atactic precursors such as poly(vinyl acetate) (PVAc), suggesting that tacticity of PVA played a paramount role in the fibrillation process. That is, fibrillation did not occur with atactic PVA because it required a certain level of crystallinity to stabilize the fibrils.[6]

The PVA fibril thus prepared has very unique features in microstructure.[3,6,9] The fiber structure is totally different from those of conventional man-made fibers prepared by spinning. Although the dimensions of the fiber varies with saponification conditions including geometry and speed of stirring and chemical nature of the precursor polymer in a very complicated manner, diameters of the fiber generally range from 1 to 100 μm, and length of the fiber is up to about 100 cm.[17] As a rule, the tensile strength of the PVA fibril was increased with increasing molecular weight, syndiotactic diad (S-diad) content, degree of saponification (DS), and degree of crystallinity of PVA. The PVA fibril having number-average degree of polymerization (P_n) of 16 700 (number-

10.1021/ma001624s CCC: $20.00
Published on Web 03/16/2001

average molecular weight of 734 800) has very high tensile strength up to 15.4 g/d without an additional chain-orientation procedures such as drawing and heat treatment.[3]

There is much research in the X-ray diffraction analysis of atactic and syndiotactic PVA fibers,[6,8,18,19] films,[12,20] gels,[13,21] and crystal mats.[22] And, we have previously reported on the basic structure and properties of the PVA fibril prepared from the saponification of PVPi and P(VPi/VAc) copolymer to PVA.[3,6,9] However, X-ray analysis of fibrillar structure formed by phase separation with increasing DS during the saponification under shearing force is rare up to now. That is, there has been no research regarding for the investigation of the structure variations of PVA fibril with stereoregularity (syndiotacticity).

In this study, to identify the influence of tacticity of PVA on the crystalline and microstructures of the novel PVA fibril, wide- and small-angle X-ray analyses of PVA fibrils having different stereoregularities and preparation histories were tried. Also, to effectively compare the shear-induced crystals in HMW syndiotactic PVA fibril with the thermal induced crystals (general crystallization method) in PVA fibril, structures of PVA fibrils formed by thermal treatment and extension (drawing at high temperature), which is able to maximize the mechanical and physical properties of the PVA fibril, were characterized in terms of syndiotacticity.

Experimental Section

Synthesis of Precursor for PVA. To synthesize the HMW syndiotactic PVPi having S-diad content of 65.1%, vinyl pivalate (VPi) was solution polymerized in *tert*-butyl alcohol at 25 °C with 2,2′-azobis(2,4-dimethylvaleronitrile) (ADMVN) as an initiator.[23] For 63.1% PVA specimen, VPi was photo-bulk-polymerized on irradiation with ultraviolet radiation with ADMVN as a photoinitiator at 10 °C.[4] Also, to obtain HMW PVPi having S-diad contents of 58.4% and 56.2%, VPi and vinyl acetate (VAc) were bulk-copolymerized at 30 °C with ADMVN as an initiator varying monomer feed ratio.[6] PVPi and P(VPi/VAc) were purified by reprecipitation in acetone/water and methanol/water, respectively. The intrinsic viscosity ([η]) of PVPi was determined in acetone at 25 °C. In the case of P(VPi/VAc), [η] was measured in benzene at 30 °C.[3,4,6]

Saponification and in-Situ Fibrillation. The fibrillation of PVA during saponification of PVPi depends on the molecular weight, the degree of syndiotacticity, and the saponification conditions (solvent, concentration, temperature, time, presence or absence of oxygen, stirring geometry, and stirring speed).[3,16,17] The conditions used in the present work were those judged to be optimum for saponification of PVPi.[3,4,16,17] PVPi or P(VPi/VAc) copolymer (4 g) was dissolved in tetrahydrofuran (200 mL), and a solution of potassium hydroxide (5 g) in methanol/water solution (90/10 v/v; 20 mL) was added drop-by-drop while stirring using an H-shaped anchor-type stainless steel stirrer at 20 000 rpm at 60 °C. (No stirring resulted in incomplete saponification, and the higher stirring rates resulted in the breakup of the gel structure that appears to be necessary for fibrillation.) After the saponification reaction was complete, the solid fibrillar reaction mixture was beaten mechanically or treated in an ultrasonic generator containing methanol. The fibers thus produced were filtered, washed several times with methanol, and dried in a vacuum. A quantitative yield of bright-yellow PVA fibrils was obtained. Figure 1 shows surface morphologies of PVA fibril with S-diad content of 65.1%. Residual ester groups could not be detected in the ^{1}H NMR spectra of these specimens.

Zone Drawing of PVA Fibril. Zone drawing was carried out at 230 and 250 °C by moving a pair of narrow band heaters with dimensions in length of 7 cm, in width of 2.5 cm, and in thickness of 1 mm along the PVA fibril.[12,24−28] The fibril was drawn under tensions controlled by different dead weights on an Instron model 4201. For obtaining PVA fibrils with different draw ratios (different degrees of crystal orientation) used for X-ray analysis, crosshead speed was controlled from 10 to 200 mm/min.

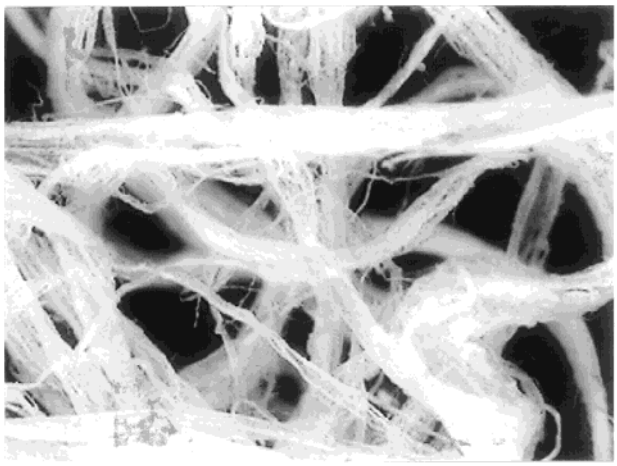

Figure 1. Optical micrograph of undrawn PVA fibril with S-diad content of 65.1%.

Characterization of PVA Fibril. The P_n of the PVAs were determined from the viscosities of the benzene solutions of the fully acetylated specimens.[3,4] The S-diad contents of the PVAs were determined by 300 MHz ^{1}H NMR, using dimethyl-d_6 sulfoxide (DMSO-d_6) as the solvent, based on the ratio of the components of the hydroxyl proton triplet at 4.1−4.7 ppm.

The surface morphology of the PVA specimens was investigated using a Scalar VMS 3000 video microscope with a magnification of ×200.

Wide-angle X-ray diffraction (WAXD) and small-angle X-ray scattering (SAXS) data were recorded on Kodak direct exposure X-ray film using Ni-filtered Cu Kα radiation and pinhole collimation. The sample-to-film distances were 55 and 315 mm for WAXD and SAXS, respectively. The exposure times for WAXD and SAXS were 12 and 48 h, respectively. The specimens were parallel bundles of 3−5 fibers. The degree of orientation of the crystallite regions was determined using the Hermans equation, based on the azimuthal half-width of the meridional reflection on the second layer line measured using an optical densitometer. $\theta/2\theta$ diffractometer scans were recorded using a Phillips PN 3550 diffractometer with scintillation counter in the transmission mode. These data were collected with increments of 0.02° ($\Delta 2\theta$) with a counting time of 30 s for each step. Cu Kα radiation was used in all measurements. The apparent crystallite size $D_{(020)}$ was estimated using Scherrer's equation:

$$D_{(020)} = \lambda/\beta \cos \theta \qquad (1)$$

where λ is an X-ray wavelength, θ is the Bragg angle of the reflection, and β is the pure integral width of the reflection. Silicon powder was used as standard sample to evaluate the instrumental broadening. The long period was obtained from the scattering angle of the SAXS meridional maximum.

PVA densities were determined using a benzene−carbon tetrachloride density gradient at 30 °C. The degree of crystallinity (X_c) was derived from eq 2:

$$1/d = X_c/1.345 + (1 - X_c)/1.269 \qquad (2)$$

where d is the measured density and 1.345 and 1.269 g/mL are the densities of the crystalline[29] and amorphous[30] PVA, respectively. The crystal melting temperature (T_m) was measured using a Perkin-Elmer, DSC 7 differential scanning calorimeter with a sample weight of 10 mg and at a heating rate of 10 °C/min.

Stress−strain curves for the fiber specimens were obtained using an Instron model 4201, with a sample length of 3 cm

Table 1. Characteristics of Undrawn PVA Fibrils Used

	S-diad content (%)			
	65.1	63.1	58.4	56.2
P_n	8200	7900	8200	7800
DS (%)	99.9	99.9	99.9	99.9
degree of crystal orientation	0.902	0.887	0.882	0.823
crystallinity (%)	52.1	49.4	47.5	45.2
T_m by first heating (°C)	263.5	261.2	252.9	248.1
T_m by second heating (°C)	251.4	248.2	239.6	236.8

and a cross-head speed of 10 mm/min. The specimens appeared very similar to those of native cellulose, notably ramie, jute, and linen, so, in calculating tensile strength of the PVA specimens, we used similar method adopted in the calculation of the tensile properties of these cellulose fibers.[31] As a fibril dimension, denier was used. The tensile strength was taken as the average of 30 measurements.

Results and Discussion

Physical Properties of Undrawn PVA Fibril. Table 1 shows some characteristics of untreated PVA fibrils with syndiotacticity. To clarify the effect of syndiotacticity on the structure and properties of the PVA fibril, we exclude molecular weight effect of the PVA fibril. In this study, by dint of the optimum combination of complex polymerization factors such as type of polymerization, polymerization temperature, initiation method, and initiator concentration, it was possible to control the P_n of the PVA fibril to a similar value of about 8000.

The higher the S-diad content of the PVA fibril, the more highly oriented the PVA fibril, and the degree of crystal orientation of the fibril with S-diad content of 65.1% was 0.902. Although the general preparation steps of high strength and high modulus PVA fibers such as spinning, drawing, and heat treatment, etc., were not conducted, a degree of crystal orientation of about 0.9 could be obtained by saponification under shearing force. Also, a crystallinity of over 45% was obtained in all of the PVA fibrils. Especially, in the case of the PVA fibril having S-diad content of 65.1%, the crystallinity was 52.1%. The PVA fiber should be heat-treated or hot drawn to acquire such a value in general PVA fiber preparation process. A reason for this high crystallinity of the fibril might be that there occurred not thermo-induced but shear-induced crystallizations of highly syndiotactic PVA chains. T_m's of the PVA fibrils by first and second heatings are listed in Table 1. It was shown that the T_m's by the first and second heatings of the fibrils with relatively higher S-diad content was larger than those of the fibrils with lower S-diad content, and this result corresponds fairly well to the previous crystallinity data. T_m of the fibril with S-diad content of 65.1% by the first heating was 263.5 °C. In fact, this value is similar to that[32] of the high strength and high modulus PVA filament obtained via the spinning of the HMW syndiotactic PVA solution in DMSO and subsequent high temperature drawing with a high draw ratio of 18 times. However, it is quite apparent that the PVA fibril having a high T_m could be prepared by the saponification and in-situ fibrillation under shearing force without additional treatments.

Microvoid Structure in PVA Fibril. It has been known that X-ray diffraction studies at low angles is an effective tool in identifying the microstructure of crystalline polymers at levels above that of the unit cell. Thus, to investigate a correlation between the microfibrillar structure and the tacticity of the PVA fibril, we used the SAXS technique. Figure 2 is the SAXS photographs of fully saponified PVAs having different syndiotacticities. All the photographs of the fibrils present the different shaped diffuse scatterings on the equator, which have maximum intensity at an angle of 0° and decrease in intensity out to 1−2°. In the cases of artificial fibers as well as natural cellulose fibers, diffuse scattering patterns similar to those in Figure 2 had been observed, and these scatterings could be interpreted as being caused by microvoids or pores in the fibers.[22,33−35] These diffuse scatterings may be ascribed to inhomogeneities of electron density.

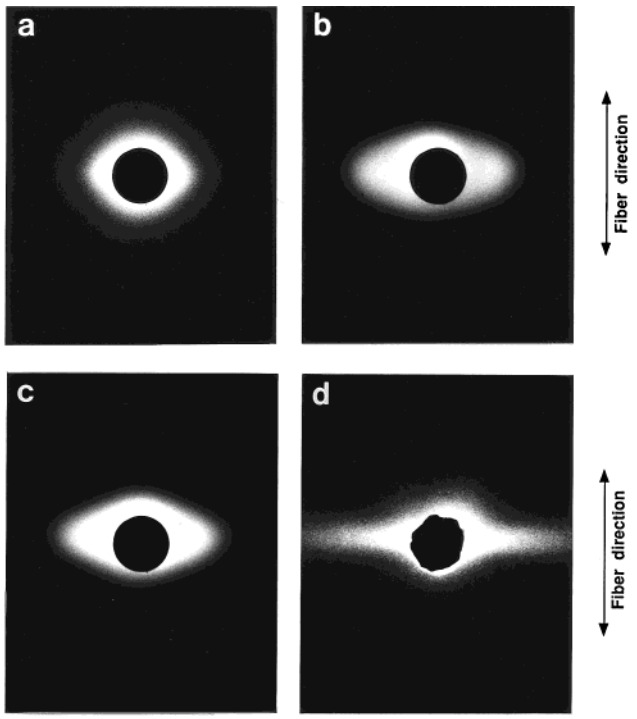

Figure 2. Small-angle X-ray scattering photographs of four undrawn PVA fibrils. S-diad content: a, 56.2%; b, 58.4%; c, 63.1%; d, 65.1%.

Factors affecting the shape of the diffuse scattering on the equator of fiber were known as the spinning method of the fiber (dry, wet, or melt), spinning solvent, methods of annealing, sintering, and drawing, etc.[22,33−35] The PVA fibril, however, is prepared not from the spinning, drawing, and heat treatment processes, the general preparation steps of synthetic fibers, but from the saponification procedure under shearing force. Therefore, it was postulated that tacticity, phase separation, and shearing force might have a influence on the shape of the diffuse scattering patterns of the fibrils. At S-diad content of 56.2% (Figure 2a), weak void scattering appeared on the equator. In contrast, in the case of 58.4% specimen, strong circular-shaped diffuse scattering was observed on the equator, and in the case of S-diad content of 63.1%, strong diamond-shaped diffuse scattering appeared on the equator. The SAXS pattern was converted to a strong line scattering parallel to the equator for 65.1% specimen, resulting from different syndiotacticities. The circular-shaped microvoid scattering in Figure 2b is similar to that from cellulose acetate fiber, and the diamond-shaped microvoid scattering in Figure 2c is similar to that from ramie fiber or drawn synthetic fiber, i.e., solution spun and drawn polyacrylonitrile fiber.[33−35] Also, strong line scattering on the equator of 65.1% PVA fibril was

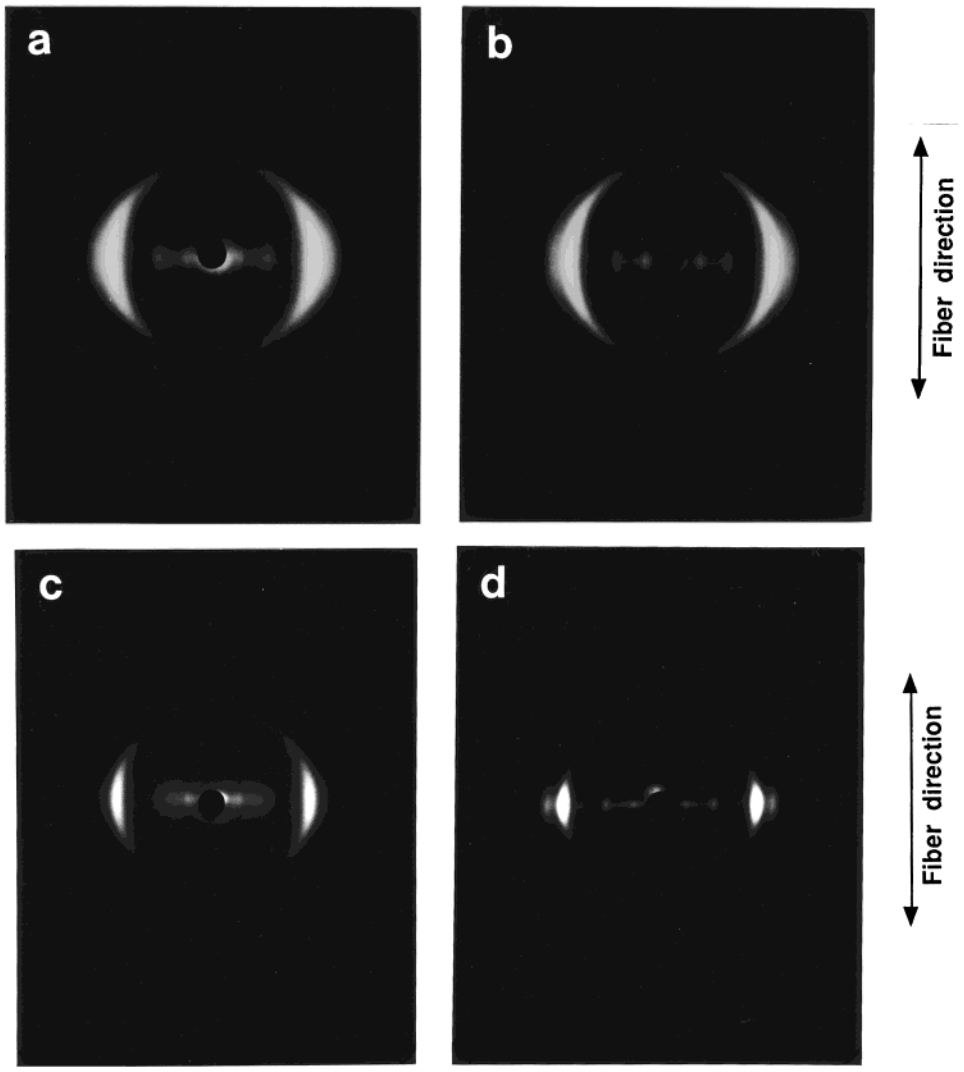

Figure 3. Wide-angle X-ray diffraction photographs of four undrawn PVA fibrils. S-diad content: a, 56.2%; b, 58.4%; c, 63.1%; d, 65.1%.

similar to that of bamboo fiber having a very fast crystallzation rate. It was known that the sharper the shape of the equator scattering, the more regular and more elongated the microvoids.[22,33−35] Thus, it was supposed that the higher the syndiotacticity was, the more regular and elongated the microvoids in PVA fibril were. This might be explained by a better alignment of PVA chains with higher syndiotacticity.

Diffuse scattering patterns similar to those in Figure 2c,d have been found in the fairly drawn synthetic fiber.[35] Because the PVA fibrils were not prepared from spinning and drawing, general physical treatments for enhancing orientation and packing properties of synthetic fiber, it was identified that the PVA fibrils with higher S-diad contents had a high internal regularity along the fiber direction, comparable to the case of the drawn synthetic fiber. The driving force which supplies high regularity described above might be a strong intermolecular hydrogen bondings of highly syndiotactic PVA chains.

Nagura et al.[36] investigated the wavenumber of the infrared absorption to the OH stretching in the crystalline region of PVA as a function of temperature. They found that the wavenumber shifted to a high frequency with temperature owing to the weakening of hydrogen bonds, and this tendency is more enhanced above 120 °C for atactic PVA and syndiotacticity-rich PVA with S-diad content of 54%. In contrast, the wavenumber shifted only monotonically with temperature for PVA with S-diad content of over 60%. They explained that this effect was ascribed to the tight intermolecular hydrogen bonds of highly syndiotactic PVA. Also, Nakamae et al.[19] found the difference of the temperature dependence of the elastic modulus of crystalline regions and the lattice spacing and diffraction intensity for the (020) plane of PVAs with S-diad contents of 55.4% and 63.0%, respectively. They concluded that the molecular motion of PVA with 63.0% is restricted because of strong intermolecular hydrogen bonds. These previous results well support our SAXS data.

Figure 3 presents the WAXD photographs of four saponified PVAs having different stereoregularities. It was shown that as the S-diad content of the PVA fibril increased, the crystal orientation increased.

Zone Drawing Behavior of PVA Fibril. In general, the zone drawing technique,[12,24−28] a method inducing a necking on one point of a fiber by heat, has many advantages compared to a hot drawing such as fewer probabilities of microcrystallities formation, of backfolding of molecular chains, and of thermal degradation of sample. Owing to the above reasons, to effectively orient the molecular chains of syndiotacticity-rich HMW

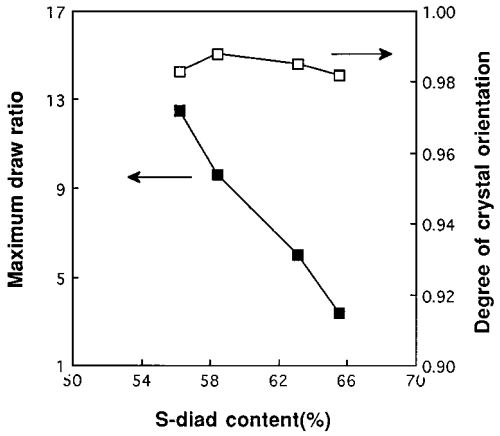

Figure 4. Relationship between maximum zone draw ratio and degree of crystal orientation of PVA fibrils with different syndiotacticities.

PVA fibril, the zone drawing technique was applied.

Commonly it has been known that the maximum draw ratios of PE and atactic PVA fiber are influenced by the molecular weight of polymer.[37−40] In other words, the higher the molecular weight, the larger the draw ratio. And PVA fibrils is a HMW PVA with P_n of about 8000. Thus, in this study, first, drawing at room temperature (first in two-stage drawing) prior to hot drawing (second in two-stage drawing) was tried to maximize draw ratio of the fibril. However, it is completely impossible to draw the fibril at room temperature nevertheless of the HMW of the fibril. The reason might be supposed that the fibril had a strong intermolecular hydrogen bond due to a higher stereoregularity and a well-oriented and crystallized microfibrillar structure. These may suppress the chain slippage in oriented morphologies, resulting in a negligible effect of molecular weight on room temperature. Owing to the above reasons, high temperature-zone drawing was directly tried at 230 and 250 °C without one-stage drawing at room temperature. At these high temperatures for syndiotactic PVA fibril, it is possible that the molecular motions in both amorphous and crystalline regions are highly activated. Thus, the intermolecular slippage may be much easier than at room temperature.

Figure 4 shows effect of syndiotacticity on the maximum zone draw ratio and degree of crystal orientation of PVA fibrils drawn at 230 °C. The draw ratio increased with a decrease in the S-diad content. Also, the maximum value up to 12.5 could be obtained at S-diad content of 56.2%. This result can be explained that flexibility of molecular chains increases with decreasing syndiotacticity above glass transition temperature. The draw ratio (deformability) of polymeric fibers varies with molecular weight, linearity, and stereoregularity of polymers, preparation and drawing conditions of fibers, etc. In this study, however, those factors except stereoregularity were negligible because same types of polymer with same molecular weight, and same preparation methods were used in all experiments. So, the higher the syndiotacticity was, the lower the draw ratio was. The reason might be explained by different stability of crystals due to different intermolecular hydrogen bonds in syndiotacticity-rich PVA, which may act as net points in both amorphous and crystalline regions, and reduces the ability of chain slippage and unravelling of crystalline lamellae. Moreover, this intermolecular hydrogen bonds restricting the molecular slippage is stronger in higher syndiotactic PVA. On the other hand, nearly the same degrees of crystal orientation of 0.982−0.988 could be obtained regardless of different draw ratios. Namely, when the same draw ratio was applied to the fibrils, higher molecular orientation was achieved for the fibrils having higher syndiotacticity (Table 2). A larger crystal orientation for higher syndiotactic PVA at the same draw ratio may be primary due to a higher efficiency of draw in PVA.

Table 2. Draw Ratio and Degree of Crystal Orientation of the PVA Fibril with Syndiotacticity

S-diad content (%)	drawing temp (°C)	draw ratio	deg of crystal orientation
56.2			0.823
56.2	200	6.4[a]	0.958
56.2	230	12.5[a]	0.983
58.4			0.882
58.4	200	3.9[a]	0.961
58.4	230	3.4	0.927
58.4	230	6.7	0.963
58.4	230	9.6[a]	0.988
63.1			0.887
63.1	230	1.8	0.923
63.1	230	3.9	0.967
63.1	230	6.0[a]	0.985
63.1	250	1.5	0.915
63.1	250	2.9	0.963
63.1	250	5.2	0.984
63.1	250	6.9[a]	0.991
65.1			0.902
65.1	230	3.4[a]	0.982
65.1	250	4.5[a]	0.990

[a] Maximum draw ratio obtained at each syndiotacticity and drawing temperature.

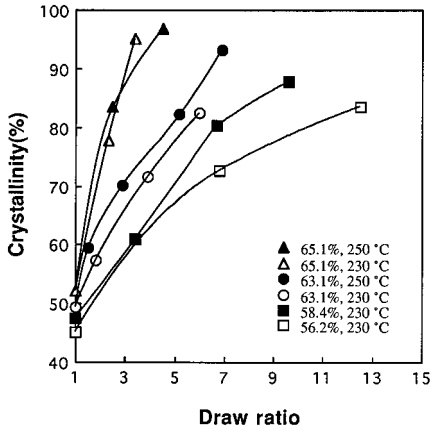

Figure 5. Crystallinity of PVA fibril with draw ratio.

Figure 5 shows the effect of syndiotacticity of the PVA fibril on crystallinity. The crystallinity increased in accordance with an increase in the S-diad content. This implies that the syndiotacticity has a marked influence on the shear-induced crystallization of the PVA during the saponification and in-situ fibrillation and on the thermal-induced crystallization of the PVA fibril. By high temperature zone drawing, a fairly high value of over 95% was obtained in the cases of 63.1 and 65.1% PVA specimens.

Relation between Long Period and Longitudinal Crystal Size. The equatorial intensity curves of the PVA fibrils with S-diad contents of 63.1% (a) and 58.4% (b) drawn at same temperatures are shown in Figure 6. Two fibrils had similar degrees of crystal orientation of 0.985 and 0.988. Nevertheless, in the case of S-diad content of 58.4%, the peak for the $(10\bar{1})$ plane at 19°

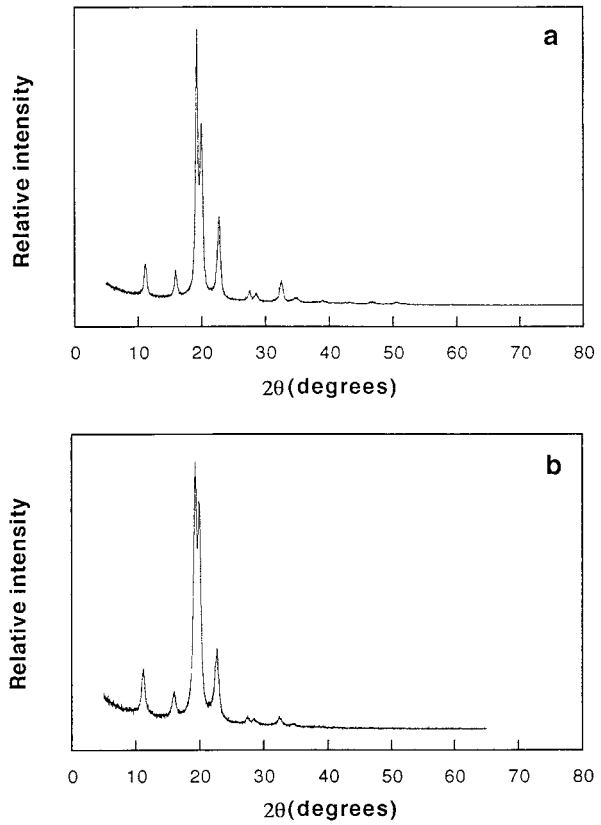

Figure 6. X-ray diffractometer-equatorial scan of PVA fibrils maximum drawn at 230 °C. S-diad content: a, 63.1%; b, 58.4%.

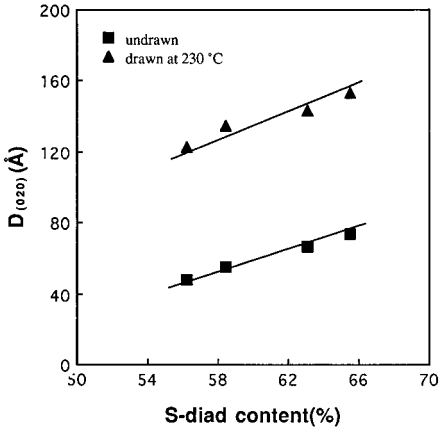

Figure 7. Tacticity dependence of the $D_{(020)}$ of PVA fibril.

was overlapped with that for (101) plane around 20° to some extent, while in the case of higher syndiotactic fibril, two peaks are much narrower, more symmetrical, and more separated. In addition, the other peaks including (100), (001), and (200) plane peaks much sharper than those of fibril with 58.4%. Thus, this explain the fact that larger crystals on lateral direction could be formed in higher syndiotactic PVA.

In this study, for more precise identification of the effects of syndiotacticity and physical treatment (drawing at high temperature) on the crystal size of the fibril, the longitudinal crystal size for (020) plane was measured from the meridional intensity curves. The crystallite size $D_{(020)}$ of the PVA fibrils with different syndiotacticities was calculated using eq 1. Figure 7 shows tacticity dependence on the $D_{(020)}$ of the PVA fibrils. Values of undrawn PVA fibrils having degrees of crystal orientation of 0.823−0.902 were about 48−74 Å. By zone

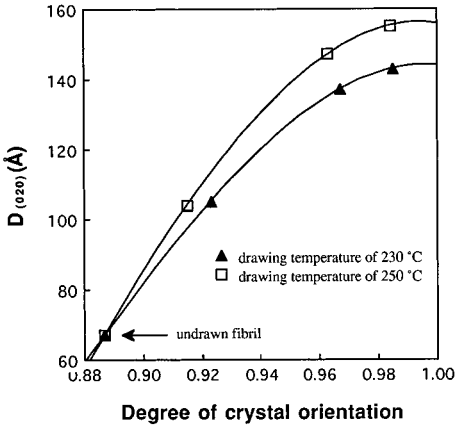

Figure 8. Degree of crystal orientation and drawing temperature dependences of the $D_{(020)}$ of PVA fibril with S-diad content of 63.1%.

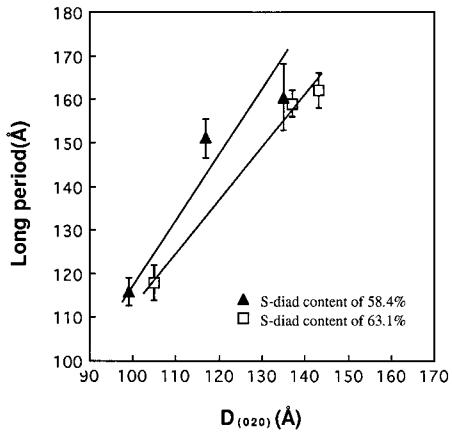

Figure 9. Relationship between long period and $D_{(020)}$ of PVA fibril drawn at 230 °C.

drawing at high temperatures, the degree of crystal orientation and $D_{(020)}$ of the fibril remarkably increased to 0.982−0.988 and to 123−153 Å, respectively. Also, in both cases, the $D_{(020)}$ was increased with an increase in the S-diad content. The effects of degree of crystal orientation and drawing temperature on the $D_{(020)}$ of the PVA fibril with S-diad content of 63.1% are presented in Figure 8. Two things are worth noting in this figure. First, the $D_{(020)}$ of the PVA fibril increased with an increase in the degree of crystal orientation. Second, the differences in the $D_{(020)}$ between 230 and 250 °C increased with an increase in the degree of crystal orientation. These facts explain that the drawing temperature of highly stereoregular PVA chain as well as syndiotacticity is an important factor in leading to the effective crystal formation. Especially, in the case of the fibril with degree of crystal orientation of 0.991 drawn at 250 °C, the highest value of about 155 Å was obtained.

The relation between long period and $D_{(020)}$ of the PVA fibril drawn at 230 °C is shown in Figure 9. Generally, the values of the long period are larger than the longitudinal crystallite size. Thus, subtraction of the crystal size from the long period can yield a deduced amorphous length, provided that a model consisting of alternating crystalline and amorphous regions in the direction of the fiber axis is assumed. Figure 9 shows value of slope of the straight line for S-diad content of 63.1% is smaller than that of 58.4%, indicating that crystal-to-amorphous lengths in long period (crystal

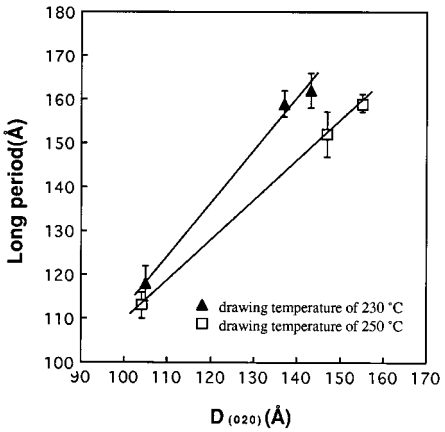

Figure 10. Relationship between long period and $D_{(020)}$ of PVA fibril with S-diad content of 63.1%.

contribution) is larger in higher syndiotactic PVA. Figure 10 presents relation between long period and $D_{(020)}$ of the drawn PVA fibril having S-diad content of 63.1%. As the fibril was drawn at higher temperature, the amorphous length was more reduced.

Effect of Syndiotacticity on the Structure of Drawn Fibril. Figures 11 and 12 show SAXS and WAXD patterns of the PVA fibril having S-diad content of 63.1% drawn at 230 °C with degree of crystal orientation, respectively. The SAXS and WAXD patterns of undrawn fibril in Figures 2c and 3c present that the molecular chains are slightly oriented and the regularly distributed microvoid along the fiber axis was formed due to a high syndiotacticity. On drawing the PVA fibril, the chain orientation proceeded rapidly along the draw direction, as shown by a series of WAXD patterns in Figure 12. The SAXS pattern of PVA fibril with degree of crystal orientation of 0.923 (Figure 11a) shows a strong long period scattering (116−122 Å) on the meridian, extended perpendicular to the fiber axis, indicating the lamellar structure formed by high-temperature zone drawing. By an increase of the degree of crystal orientation to 0.967 (Figure 11b), the long period increased to 156−162 Å, and the length of the streak across the meridian was shortened. This means that the lamellar width are broader: a plane or network lattice rather than a line lattice. This result well agrees that the length of this streak is inversely related to the width of the superlattice region, reported by Hess and Kiessig.[41] In contrast, in the case of S-diad content of 58.4% in Figures 13 and 14, a longer streak across the meridian was observed at degree of crystal orientation of 0.963

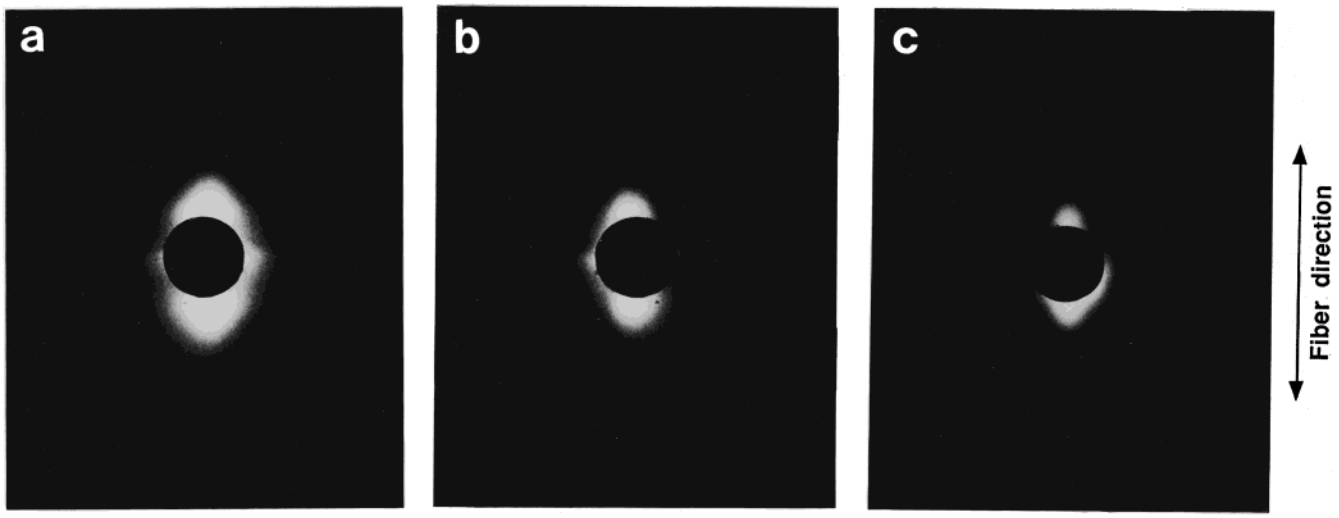

Figure 11. Small-angle X-ray scattering photographs of PVA fibrils with S-diad content of 63.1% drawn at 230 °C. Degree of crystal orientation: a, 0.923; b, 0.967; c, 0.985.

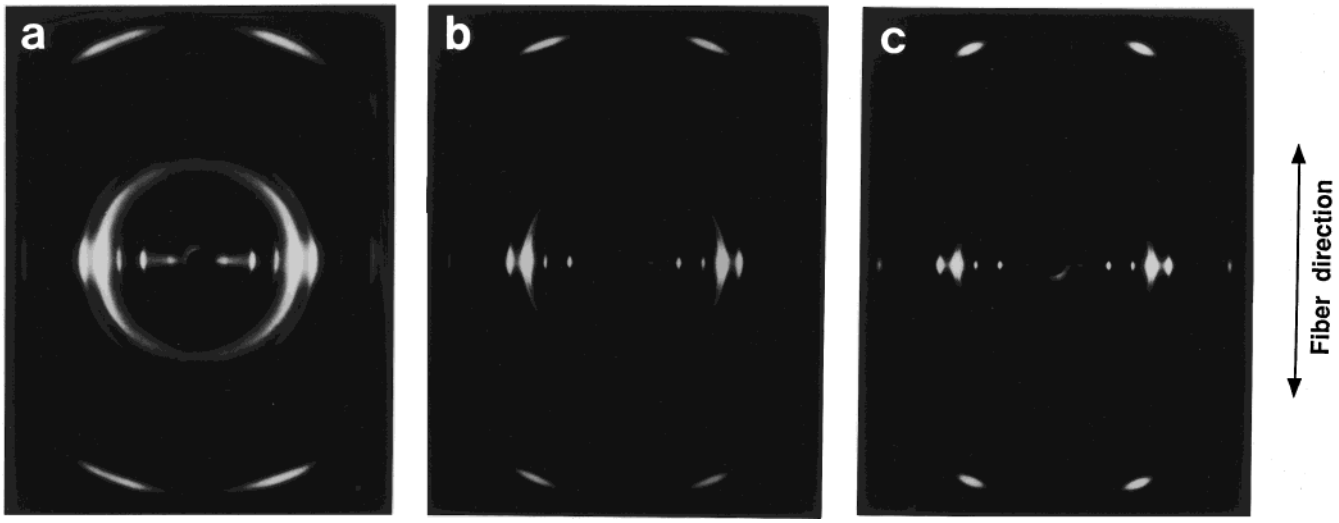

Figure 12. Wide-angle X-ray diffraction photographs of PVA fibrils with S-diad content of 63.1% drawn at 230 °C. Degree of crystal orientation: a, 0.923; b, 0.967; c, 0.985.

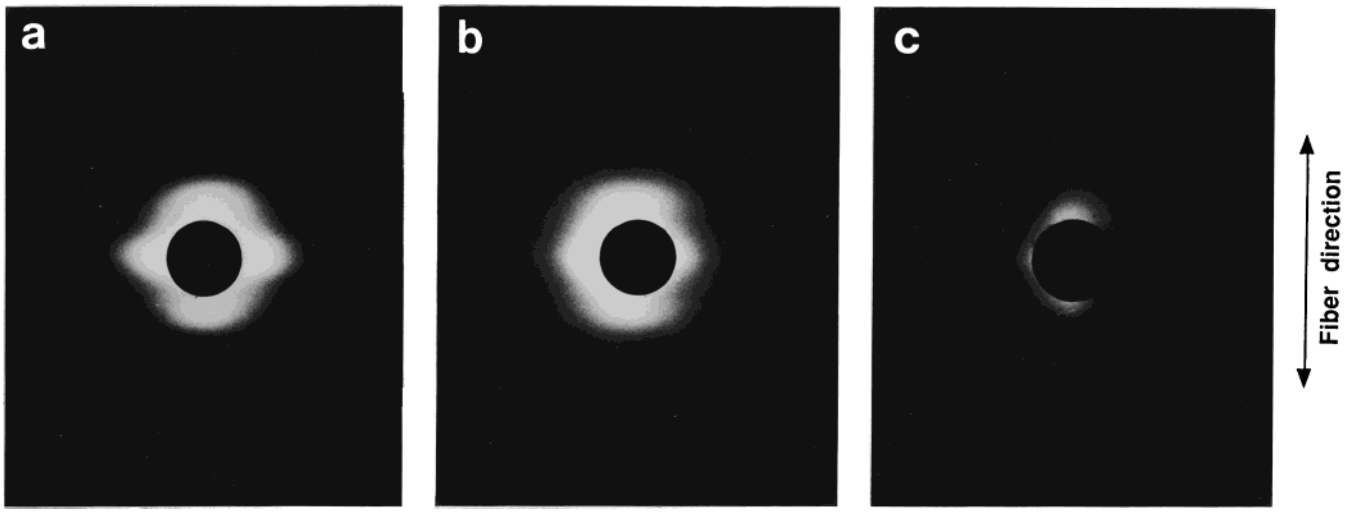

Figure 13. Small-angle X-ray scattering photographs of PVA fibrils with S-diad content of 58.4% drawn at 230 °C. Degree of crystal orientation: a, 0.927; b, 0.963; c, 0.988.

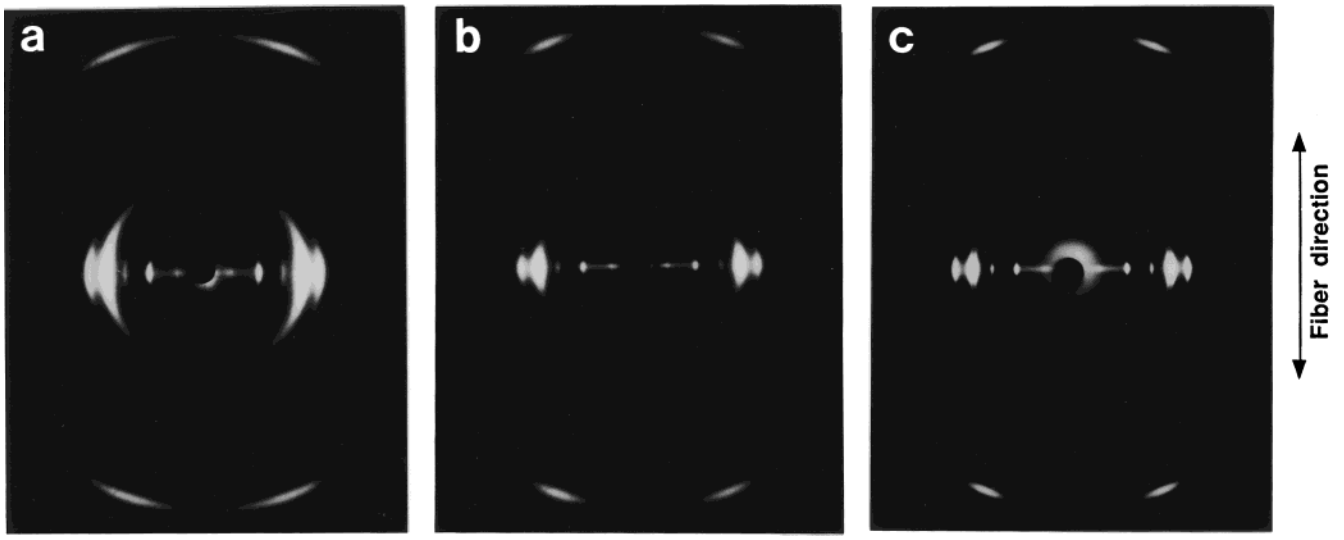

Figure 14. Wide-angle X-ray diffraction photographs of PVA fibrils with S-diad content of 58.4% drawn at 230 °C. Degree of crystal orientation: a, 0.927; b, 0.963; c, 0.988.

(Figure 13b) in comparison with that of S-diad content of 63.1%. This means that with increasing syndiotacticity, there is an increase in the dimension of the crystal lamellae.

The scattering intensity decreased with increasing degree of crystal orientation of both 63.1% and 58.4%. At a degree of crystal orientation of 0.985 of PVA with S-diad content of 63.1%, the long period scattering became negligibly weak even for a long exposure time of 48 h, as shown in Figure 11c. In addition, this phenomenon is more obvious in the case of 58.4% in Figure 13c. Such a decrease in intensity with increasing draw ratio (degree of crystal orientation) has been reported on drawing polyethylene (PE).[42] The critical draw ratio, above which the intensity of long period scattering approaches zero, has been found to be about 80 for drawing ultrahigh molecular weight (UHMW) PE fiber, depending on the drawing conditions and techniques used.[42] The corresponding draw ratios for PVA fibrils having S-diad contents of 63.1% and 58.4% are respectively 6.0 and 9.6. Although the SAXS intensity depends on several structural parameters, such a draw ratio may be understood as the draw ratio above which the initial amorphous−crystalline two structures approache a one-phase structure, in which the defects including the residual folds, trapped entanglements, chain ends, etc., are distributed more or less randomly. When the density difference between the two phases is small, as in the case for poly(4-methylpentene-1) at room temperature, the SAXS pattern never appears, even if the long period is well formed by alternately stacked crystalline and amorphous phases.[43] The density contrast generally tends to decrease with drawing, because the packing density in the amorphous phase is increased with drawing, while that of the crystalline phase remains almost constant. In the case of syndiotactic PVA, however, it is supposed that the amorphous density cannot increase so much that the density difference becomes small enough to make the SAXS pattern disappear, since the packing density is very high in the crystal phase. It should be remarked that the small density contrast in poly(4-methylpentene-1) is attributed to the extraordinary low density of the crystal.[43] This consideration leads us to conclude that vanishing of the scattering pattern in Figure 13c is due to the destruction of the long period. From these results, it is concluded that the alternately stacked crystalline and amorphous two-phases structure is destroyed dur-

ing the uniform zone drawing after necking and is reorganized into a single-phase crystalline structure. The fact that the critical draw ratio for syndiotactic PVA with S-diad content of 63.1% is small compared with that with S-diad content of 58.4% suggests a higher efficiency of draw for the former polymer. This result is well coincident with the previous maximum zone draw ratio data. In comparison with Figure 13c, Figure 11c shows a trace that amorphous−crystalline two structures remains. This might be explained by differences of chain rigidity and crystal stability of two syndiotacticity-rich PVA specimens. Because the chains in PVA with 63.1% is more rigid than that with 58.4% and the crystal in 63.1% PVA is more stable than that in 58.4% specimen, it is more difficult for PVA chains with 63.1% to be extended at the same drawing temperatures.

By drawing all the PVA fibrils with tensile strength of 8−20 g/d, a tensile strength of over 30 g/d was obtained. In particular, the strength of the fibril having S-diad content of 63.1% reached the very high value of over 45 g/d (5.5−6.0 GPa). This level of tensile strength is comparable to that of graphite fiber which exceeds the maximum tensile strengths of Kevlar and Technora fibers (3 GPa), UHMW PE fiber (Spectra, 5 GPa), and poly(*p*-phenylene benzobisthizole) fiber (3 GPa).[44,45] The reason is that the PVA fibril has a high syndiotacticity, a HMW, and a well-packed ultrafine microfibril structure formed by strong intermolecular hydrogen bonding and represents one of the most crystalline of all fibrous polymers, which was prepared by high-temperature zone drawing.

Conclusions

Investigating the effects of syndiotacticity on the crystal and microstructures of the PVA fibrils prepared from the saponification and in-situ fibrillation without spinning procedure by SAXS and WAXD analyses, we may conclude the following: It was found that PVA fibrils had various microvoid structures with different stereoregularities, similar to those observed in various natural cellulose fibers. And, the regularities of these microvoids along the fiber direction were increased with an increase in the syndiotacticity, indicating that syndiotacticity played a significant role in alignment of PVA chains. The degree of crystal orientation to 0.991 was achieved by stretching the PVA fibril with S-diad content of 63.1% and with original degree of crystal orientation of 0.887 at around 250 °C close to its crystal melting temperature. The maximum draw ratio of the PVA fibril increased with a decrease in the S-diad content. Namely, as syndiotacticity was increased, so the deformability (drawability) of PVA chains was lowered. This is ascribed to a difference of crystal stability between PVA fibrils having different stereoregularities. Higher crystal orientation was achieved for the fibrils having higher syndiotacticity of PVA at the same draw ratio. The crystallinity, the apparent lateral and longitudinal crystal sizes, and the crystal-to-amorphous length in a long period of drawn PVA fibrils were larger in higher syndiotacticity. The PVA fibril drawn at 230 °C had a well-oriented lamellar structure, and dimensions of these lamellae were enlarged with increasing syndiotacticity. Conclusively, it was identified that syndiotacticity had a fundamental effect on the structure of the PVA fibril.

Acknowledgment. This research was supported by Yeungnam University research grants in 2000.

References and Notes

(1) Marten, F. L. In *Encyclopedia of Polymer Science and Engineering*; Mark, H. F., Bikales, N. M., Menges, C. G., Kroschwitz, J. I., Eds.; Wiley: New York, 1985; Vol. 17, pp 167−180, 188.
(2) Masuda, M. In *Polyvinyl Alcohol—Developments*; Finch, C. A., Ed.; Wiley: New York, 1991; pp 403−422, 711.
(3) Lyoo, W. S.; Ha, W. S. *Polymer* **1996**, *37*, 3121.
(4) Lyoo, W. S.; Ha, W. S. *J. Polym. Sci., Polym. Chem. Ed.* **1997**, *35*, 55.
(5) Lyoo, W. S.; Kim, B. C.; Ha, W. S. *Polym. Eng. Sci.* **1997**, *37*, 1259.
(6) Lyoo, W. S.; Blackwell, J.; Ghim, H. D. *Macromolecules* **1998**, *31*, 4253.
(7) Lyoo, W. S.; Kim, B. C.; Ha, W. S. *Polym. J.* **1997**, *30*, 424.
(8) Cho, J. D.; Lyoo, W. S.; Chvalun, S. N.; Blackwell, J. *Macromolecules* **1999**, *32*, 6236.
(9) Lyoo, W. S.; Ha, W. S. *Polymer* **1999**, *40*, 497.
(10) Choi, J. H.; Lyoo, W. S.; Ko, S. W. *Macromol. Chem. Phys.* **1999**, *200*, 1421.
(11) Kim, B. C.; Lyoo, W. S.; Ha, W. S. *Polym. J.* **2000**, *32*, 159.
(12) Lyoo, W. S.; Han, S. S.; Yoon, W. S.; Ji, B. C.; Lee, J.; Cho, W. W.; Choi, J. H.; Ha, W. S. *J. Appl. Polym. Sci.* **2000**, *77*, 123.
(13) Sakurada, I.; Ito, T.; Nakamae, K. *J. Polym. Sci.* **1966**, *C15*, 75.
(14) Tashiro, K.; Kobayashi, M.; Tadokoro, H. *J. Macromol. Sci.* **1977**, *10*, 731.
(15) Hess, V. K.; Steinmann, R.; Kiessig, H.; Avisiers, I. *Kolloid Z. Z. Polym.* **1957**, *153*, 128.
(16) Lyoo, W. S. Ph.D. Thesis, Seoul National University, 1994.
(17) Ha, W. S.; Lyoo, W. S.; Choi, Y. G. U.S. Patent 6,124,033, 2000.
(18) Bunn, C. W.; Peiser, H. S. *Nature* **1947**, *161*, 159.
(19) Nakamae, K.; Nishino, Y.; Ohkubo, H.; Matsuzawa, S.; Yamaura, K. *Polymer* **1992**, *33*, 2581.
(20) Matsuo, M.; Harashina, Y.; Ogita, T. *Polym. J.* **1993**, *25*, 319.
(21) Sawatari, C.; Yamamoto, Y.; Yanagida, N.; Matsuo, M. *Polymer* **1993**, *34*, 956.
(22) Kanamoto, T.; Kiyooma, S.; Tovmasyan, Y.; Sano, H.; Narukawa, H. *Polymer* **1990**, *31*, 2039.
(23) Lyoo, W. S.; Ghim, H. D. *Polymer*, in press.
(24) Han, S. S.; Yoon, W. S.; Lyoo, W. S.; Lee, C. J.; Ji, B. C.; Kim, E. K. *J. Macromol. Sci., Phys.* **1997**, *B36*, 1.
(25) Choi, J. H.; Cho, W. W.; Ha, W. S.; Lyoo, W. S.; Lee, C. J.; Ji, B. C.; Han, S. S.; Yoon, W. S. *Polym. Int.* **1998**, *47*, 237.
(26) Lyoo, W. S.; Han, S. S.; Choi, J. H.; Cho, W. W.; Ha, W. S. *J. Korean Fiber Soc.* **1995**, *32*, 1023.
(27) Lyoo, W. S.; Kim, J. H.; Yoon, W. S.; Ji, B. C.; Choi, J. H.; Cho, J.; Lee, J.; Yang, S. B.; Yoo, Y. *Polymer* **2000**, *41*, 9055.
(28) Ji, B. C.; Yoon, W. S.; Kim, S. Y. *J. Korean Fiber Soc.* **1993**, *30*, 328.
(29) Sakurada, I.; Fuchino, K.; Okada, A. *Kaken Hokoku* **1950**, *23*, 78.
(30) Sakurada, I.; Nukushina, Y.; Sone, Y. *Kobunshi Kagaku* **1955**, *12*, 506.
(31) In *Identification of Textile Materials*, 7th ed.; The Textile Institute: Manchester, 1975; pp 78−85.
(32) Fukunishi, Y.; Akiyama, A.; Sato, T.; Sano, H.; Ohmory, A. U.S. Patent 5,238,995, 1993.
(33) Statton, W. O. *J. Polym. Sci.* **1956**, *22*, 385.
(34) Kiessig, H. *Kolloid-Z.* **1957**, *152*, 62.
(35) Statton, W. O. *J. Polym. Sci.* **1962**, *58*, 205.
(36) Nagura, M.; Matsuzawa, S.; Yamaura, K.; Ishikawa, H. *Polym. Commun.* **1983**, *24*, 250.
(37) Cebe, P.; Grubb, D. T. *J. Mater. Sci.* **1985**, *20*, 4465.
(38) Kwon, Y. D.; Kavesh, S.; Prevorsek, D. C. U.S. Patent 4,440,711, 1984.
(39) Termonia, Y.; Meakin, P.; Smith, P. *Macromolecules* **1985**, *18*, 2246.
(40) Garrett, P. D.; Grubb, A. T. *J. Polym. Sci., Polym. Phys. Ed.* **1998**, *26*, 2509.
(41) Hess, K.; Kiessig, H. *Kolloid-Z.* **1953**, *130*, 10.
(42) Furuhata, K.; Yokokawa, T.; Seoul, C.; Miyasaka, K. *J. Polym. Sci., Polym. Phys. Ed.* **1986**, *24*, 59.
(43) Tanigami, T.; Miyasaka, K. *J. Polym. Sci., Polym. Phys. Ed.* **1981**, *19*, 1865.
(44) Allen, S. R.; Farris, R. J.; Thomas, E. L. *J. Mater. Sci.* **1985**, *20*, 2727.
(45) Lemstra, P. J.; van Aerle, A. J. M.; Bastiaansen, C. W. M. *Polym. J.* **1987**, *19*, 85.

MA001624S